

SOLUTION OF MULTI-CHANNEL CONTINUUM STATE PROBLEMS OF
MANY-ELECTRON ATOMIC SYSTEMS USING THE SPLINE-GALERKIN
AND INVERSE ITERATION APPROACH

By

Jinhua Xi

Thesis

Submitted to the Faculty of the
Graduate School of Vanderbilt University
in partial fulfillment of the requirements

for the degree of

MASTER OF SCIENCE

in

Computer Science

December 1996

Nashville, Tennessee

Approved:

Date:

ACKNOWLEDGEMENTS

I thank my advisor, Dr. Charlotte Froese Fischer, for her invaluable advice and guidance on my research, in both computational science and theoretical atomic physics, and for giving me the opportunity to exploit the fields of computational sciences and computer sciences.

I thank Dr. Fitzpatrick for his time in reading my thesis. I would like to express my appreciation to other faculty and staff and graduate students in the Computer Science Department. I appreciate their help to me during this degree program. I should particularly thank Mr. Andy Richter for his invaluable help in many computer related issues.

This work was supported by the Division of Chemical Sciences, Office of Basic Energy Sciences, Office of Energy Research, U.S. Department of Energy.

TABLE OF CONTENTS

	Page
ACKNOWLEDGEMENTS	ii
LIST OF FIGURES	iv
LIST OF TABLES	v
Chapter	
I. INTRODUCTION	1
II. THE <i>B</i> -SPLINE AND GALERKIN APPROACH	5
The <i>B</i> -spline basis	5
The atomic state wave function	7
The spline-Galerkin method and the interaction matrix	9
The boundary condition	12
III. CONTINUUM STATE WAVE FUNCTION AND ITS APPLICATION	13
Multi-channel inverse iteration approach	13
Normalization of wave function	14
Cross section and angular distribution	19
IV. DESCRIPTION OF THE PROGRAM PACKAGES	23
Program design and implementation strategy	23
The CHMAT program package	24
The INVPHOTO program package	25
The TOOL program package	26
Common libraries	27
Program usage	27
V. PROGRAM VALIDATION AND APPLICATION	31
Program validation methods	31
Test cases	33
Applications in atomic photodetachment processes	34
VI. FUTURE DEVELOPMENT	39
Study of many-electron systems with core polarization	39
Study of atomic auto-ionization and autodetachment processes	40
Study of electron impact processes	40
BIBLIOGRAPHY	42

LIST OF FIGURES

Figure	Page
2.1. A distribution of B -splines $B_{i,5}(x)$ in the region $x \in [0,1]$ where the horizontal coordinate labels the x value and the vertical one indicates the value of the B -splines. The 14 B -splines of order 5 are defined by the knot sequence $t_1 = \dots = t_5 = 0, t_i = t_{i-1} + 0.1$, for $i = 6, 7, \dots, 14$ and $t_{15} = \dots = t_{19} = 1$.	8
4.1. The schematic structure of the CHMAT program package	29
4.2. The schematic structure of the INVPHOTO program package	30
5.1. Comparison of the present calculation with the experimental data of Walter, Seifert, and Peterson[22] in the region of the $1s2p^2$ sharp resonance. The experimental data are scaled by a factor of $5/9$ because of the reason described in Ref[22]. We can see that the agreement is really impressive.	35

LIST OF TABLES

Table	Page
5.1. Total photoionization cross section (Mb) for the Helium 1S state. The spline parameters are: $h = 1/8$, $h_{max} = 3/8$, $R_{max} = 40.$, $k = 8$, with 16 channels. The dimension of the matrix is 2052	36
5.2. Phase shift matrix under different orthogonality scheme. 1) without overlap matrix, 2) with overlap matrix. The photon energy is 68 eV	36
5.3. K-matrix under different orthogonality scheme. 1) without overlap matrix, 2) with overlap matrix. The photon energy is 68 eV	37
5.4. Partial and total photoionization cross section (Mb) for the Helium 1S state. Degenerate solutions are obtained under two orthogonality algorithm: 1) without overlap matrix, 2) with overlap matrix. The spline parameters are the same as in Table 5.1. Initial state are from $n=5$ MCHF expansion. The photon energies are 68 eV and 75 eV, there are 4 open channels at 68 eV and 9 open channels at 75 eV. For each open channel, the first row in the table lists the results of case 1, the second row lists the results of case 2. We see the results of the two cases are identically the same.	37
5.5. The resonance parameters for the $1s2p^2\ ^4P$ sharp resonance are determined by fitting the total cross section to Eq.(3.45) in the energy region from 1.22 eV to 1.28 eV. Threshold energy was fixed in the fitting process. Other theoretical and experimental results are also listed for comparison.	38
5.6. The positions and widths of the Feshbach resonances below the $n = 3$ and $n = 4$ thresholds.	38

CHAPTER I

INTRODUCTION

Theoretical computation has been one of the most important aspects in the investigation of atomic structure and interaction. The design of efficient software packages has become an important part of the ability to perform an accurate, systematic study in this area. In the recent years, the study of the photodetachment process of negative ions has been one of the hot topics in atomic physics. In this problem, an electron in a negative ion is detached by a laser beam to continuum states. We need to design efficient software to perform accurate *ab initio* calculations of photodetachment properties, such as phase shifts, cross sections and angular distributions.

The *B*-spline method was shown to be an efficient method for representing both the bound and continuum radial orbital wave functions of an atomic state wave function[1, 2, 3]. This *B*-spline basis was combined successfully with the Galerkin approach and the inverse iteration approach to solve continuum state problems of two electron atomic systems with only one open channel[4, 5]. The Galerkin approach was used for establishing the interaction matrix whereas inverse iteration was used for solving the system of linear equations for the continuum states.

This approach was so successful that we extend it to treating general continuum state problems of many electron atomic systems. Extension is needed for the following aspects:

- For two electron systems, the target states are single configuration states. But for many electron systems, to achieve acceptable accuracy, in general, we need to build multi-configuration target states which are orthogonal to each other. So we need to extend the CHMAT package to accept multi-configuration target states.
- We need to deal with continuum states with multi-open channels instead of a single open channel. We need to find a correct and efficient way to connect the calculated continuum wave functions with the asymptotic physical solutions and get the conversion matrix(a scalar quantity in single open channel case). The old INVPHOTO package should be replaced by a new one.
- We need to extend the physics application package to deal with the multi-open channel case and add more functionality such as the calculation of the angular distribution which is a very important aspect in continuum state problems.

With the above extension included, we can classify the basic procedures involved in this calculation into the following steps:

- 1) Calculate the bound state wave function using standard atomic structure program packages [6].
 - generate the configuration list for the initial state, target states and bound perturbers of the final states, using the LSGEN package.
 - optimize the atomic orbital functions and energies using the MCHF package.

- calculate the energies and wave functions of the initial state and target states using either the MCHF package or the CI package.
 - select the bound perturber configurations if possible, by using the TOOL program package which will be described later in Chapter IV.
- 2) Use the TOOL program to compose the configuration list for the final state, which includes bound perturbers, channel configurations, and orthogonality constraints; generate the integral list using XNONH; and setup a general interaction matrix using the spline-Galerkin program package CHMAT.
 - 3) Solve for the final state wave function with given energy using inverse iteration and normalize the wave function, by using the INVPHOTO package.
 - 4) Use the TOOL program package to analyze the wave function, and study the physical properties from the wave function.

In the following chapters, we will illustrate in detail how to carry out the tasks listed above. In Chapter II we introduce the idea of the *B*-spline basis and the Galerkin approach, and their application to the continuum state problem in atomic physics. We will describe how to setup the interaction matrix from the configuration list and integral list, using the spline-Galerkin approach. Chapter III covers the topics of multi-channel inverse iteration, the normalization of the channel wave function, and the calculation of the physical properties such as cross sections and angular distributions. Chapter IV discusses the program packages, their structure and usage. Validation procedures for checking the correctness of the software package are also given in this chapter. In chapter V we give some test cases and real applications of the

program packages. We also discuss in Chapter VI the reusability of these packages and possible extensions to incorporate more functionalities in the calculation of atomic structure, interactions, and other physical phenomena.

CHAPTER II

THE B -SPLINE AND GALERKIN APPROACH

In this chapter, we will illustrate the spline-Galerkin method and its application to the calculation of atomic state wave functions. We first introduce the B -spline basis into our calculation of the continuum atomic state wave function. Then, by employing the Galerkin approach we establish the interaction matrix and apply the orbital orthogonality constraints to the matrix. Finally, we apply the boundary condition to the channel orbitals.

The B -spline basis

The B -splines are piecewise polynomials defined on a given knot sequence $\{t_i, i = 1, 2, \dots\}$. The B -splines of order K on the r axis are defined as

$$B_{i,1}(r) = \begin{cases} 1, & t_i \leq r < t_{i+1} \\ 0, & \text{otherwise,} \end{cases} \quad (2.1)$$

$$B_{i,K}(r) = \frac{r - t_i}{t_{i+K-1} - t_i} B_{i,K-1}(r) + \frac{t_{i+K} - r}{t_{i+K} - t_{i+1}} B_{i+1,K-1}(r). \quad (2.2)$$

A sample example of a set of B -splines is shown in Figure 2.1. A detailed illustration of the properties of the B -splines can be found in the book by deBoor [7].

The selection of the knot sequence is very important to the efficiency of the B -spline approach. The basic rules of setting knot sequences for atomic problems can be found in the literature[4, 5]. Generally, in the inner region of the atom, the atomic orbital wave functions scale with respect to the nuclear charge Z , so we should set the knot sequence based on $t = Zr$, where r is the radial coordinate. For the continuum

state problem, the wave function oscillates in the asymptotic region, so the spline functions should be uniformly distributed in this region. Based on these considerations, the knot sequence of a set of N splines defined on the r axis are selected as follows:

$$\begin{aligned}
t_i &= 0 && \text{for } i = 1, \dots, K \\
t_{i+1} &= t_i + h && \text{for } i = K, \dots, K + m \\
t_{i+1} &= t_i(1 + h) && \text{for } 1 < t_{i+1} - t_i < h_{max} \\
t_{i+1} &= t_i + h_{max} && \text{for } t_i < Zr_{max}; \\
&&& \text{set } N + 1 = \max(i) \\
t_{N+i} &= t_{N+1} && \text{for } i = 2, \dots, K
\end{aligned}$$

where h is the base step size, obtained from $h = 2^{-m}$, m is an integer. h_{max} is the maximum stepsize and r_{max} the maximum radial radius of the wave function, specified by the user.

The following principles are followed in selecting these parameters for a continuum state problem,

- The order of the spline basis plays an important role for the accuracy of the spline representation of the atomic wave functions. A proper selection is $K = 8$.
- r_{max} must be larger than the radius of all bound state orbitals, and must be large enough so that the minimum continuum energy of interest can be studied. Our experience indicates that this can be determined from the relation $kr_{max} \geq (3\pi \sim 5\pi)$, with $k^2/2$ being the energy of the electron in a continuum

channel, in atomic units. For the multi-open-channel case, this should be the energy of the electron in the highest open channel (with smallest k value).

- h_{max} cannot be too large, with proper K value ($K = 8$, for example), a suitable choice for h_{max} is that the biggest step size $\Delta = r_{N+1} - r_N$ satisfies the relation $k_{max}\Delta < \pi/3$, with k corresponding to that of the electron in the lowest channel, i.e., we should put at least 3 knots within a half period of oscillation of the continuum orbital wave function in the asymptotic region.

From this analysis we see that it is not appropriate to study a large energy region with many open channels by using the same knot sequence because the channel with low target energy requires a small h_{max} value whereas the channel with high target energy requires a large r_{max} value, this will lead to an interaction matrix of very large dimension.

The atomic state wave function

The continuum state wave function can be written as

$$\Psi(\gamma LS) = \sum_{i=1}^{M_p} c(i)\phi(\alpha_i LS) + \sum_{i=1}^{M_c} |(target_i \bullet | \overline{n_i l_i} \rangle) LS \rangle \quad (2.3)$$

where the first sum represents the perturber state, the second term is the channel state, represented in terms of the coupled states of the targets $| target_i \rangle$ and channel orbitals $| \overline{n_i l_i} \rangle$. The bound states $\phi(\alpha_i LS)$ and the target states $| target_i \rangle$ are defined in terms of the fixed orbitals obtained from an MCHF calculation. The $| target_i \rangle$ states are represented by multi-configuration wave functions. Orthogonality is required among all target state wave functions and all configuration state wave functions (including perturber-perturber, perturber-channel, and channel-channel).

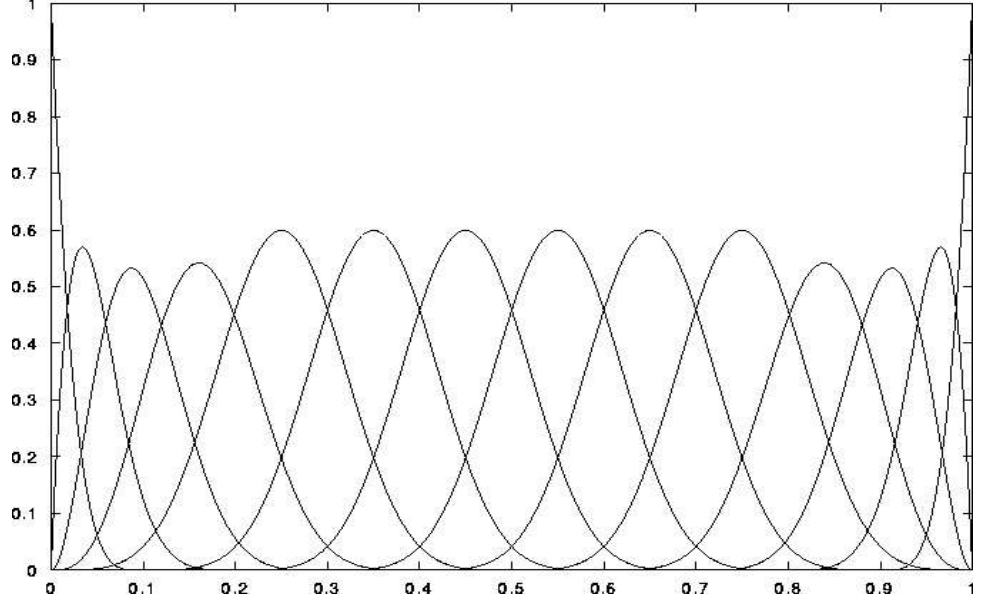


Figure 2.1: A distribution of B -splines $B_{i,5}(x)$ in the region $x \in [0,1]$ where the horizontal coordinate labels the x value and the vertical one indicates the value of the B -splines. The 14 B -splines of order 5 are defined by the knot sequence $t_1 = \dots = t_5 = 0, t_i = t_{i-1} + 0.1$, for $i = 6, 7, \dots, 14$ and $t_{15} = \dots = t_{19} = 1$.

We also require that all channel orbital wave functions be orthogonal to all fixed orbital wave functions. The orthogonality is not required among channel orbital wave functions.

The wave function in Eq.(2.3) must satisfy the Schrödinger equation

$$H\Psi = E\Psi \quad (2.4)$$

where H is the hamiltonian of the system in atomic units,

$$H = \sum_{i=1}^N \left(-\frac{1}{2}\Delta_i^2 - \frac{Z}{r_i} + \sum_{i<j} \frac{1}{r_{ij}} \right) \quad (2.5)$$

representing the interaction of an N -electron atom with nuclear charge Z . E is the total energy of the system. For a continuum state system, the energy E can be expressed as the sum of the target energies E_{t_i} and the corresponding electron energy

associated with this target, i.e.

$$E = E_{t_i} + k_i^2/2 \quad (2.6)$$

To solve the Schrödinger equation for the wave function Ψ , we approximate the wavefunction with a set of atomic configuration state wavefunctions as shown in Eq.(2.3), and we further expand the radial channel orbital wave function $P(r)$ of the atomic state wavefunction in terms of a B -spline basis set, $B_i(r)$, as

$$P(r) = \sum_j d_j B_j(r) \quad (2.7)$$

then the wave function in Eq.(2.3) can be written as

$$\Psi(\gamma LS) = \sum_{i=1}^{M_p} c_i \phi(\alpha_i LS) + \sum_{i=1}^{M_e} \sum_{j=1}^N a_j(i) |\tau_{i,j} \rangle \quad (2.8)$$

where $|\tau_{i,j} \rangle$ is the i -th channel function with the radial orbital function substituted by the j -th B -spline basis function, so that

$$|\tau_{i,j} \rangle = |(target_i \bullet | \overline{n_i l_i}(B_j) \rangle) LS \rangle \quad (2.9)$$

The spline-Galerkin method and the interaction matrix

With the wave function expanded in terms of the B -spline basis as in Eq.(2.8), we expect that under good approximation the residual (res) of the system is

$$res = (H - E)\Psi(\gamma LS) \approx 0 \quad (2.10)$$

The Galerkin condition requires that the residual be orthogonal to the solution space for a set of test functions. This is achieved by choosing a set of test functions, τ_i , that spans the solution space and requiring

$$\langle \tau_i | res \rangle = 0 \quad (2.11)$$

The test functions in the current case are

- $\phi(\alpha_i LS), i = 1, \dots, M_p$
- $|\tau_{i,j}\rangle, i = 1, \dots, M_c, j=1, \dots, N$

Applying the Galerkin condition we get the following generalized eigenvalue problem

$$(\mathbf{H} - \mathbf{E}\mathbf{S})\mathbf{C} = 0 \quad (2.12)$$

Here \mathbf{C} is the solution vector

$$\mathbf{C} = \begin{pmatrix} \mathbf{c} \\ \mathbf{a}(\mathbf{1}) \\ \mathbf{a}(\mathbf{2}) \\ \vdots \\ \mathbf{a}(\mathbf{M}_c) \end{pmatrix} \quad (2.13)$$

where \mathbf{c} is the column vector of coefficients of the expansions defining the perturbbers in Eq.(2.3) and $\mathbf{a}(\mathbf{i}), \mathbf{i} = \mathbf{1}, \mathbf{2}, \dots, \mathbf{M}_c$ is the column vector of B -spline coefficients for channel \mathbf{i} .

The interaction matrix $(H - ES)$ has the following form:

$$\begin{pmatrix} h(pp) - E\mathbf{I} & h(1p)^T & h(2p)^T & \dots & h(M_cp)^T \\ h(1p) & H(11) - E\mathbf{B} & H(12) & \dots & H(1M_c) \\ h(2p) & H(21) & H(22) - E\mathbf{B} & \dots & H(2M_c) \\ \vdots & \vdots & \vdots & \ddots & \vdots \\ h(M_cp) & H(M_c1) & H(M_c2) & \dots & H(M_cM_c) - E\mathbf{B} \end{pmatrix} \quad (2.14)$$

where \mathbf{I} is an $M_p \times M_p$ unit matrix, \mathbf{B} is the B -spline overlap matrix of dimension $N \times N$, $h(pp)$ is an $M_p \times M_p$ matrix and comes from the perturber-perturber interaction.

The $h(ip)$'s are $N \times M_p$ matrices, representing the interaction between the i -th channel and the perturber states. $H(ij)$ are $N \times N$ matrices for channel-channel interaction. The energy E of the system is determined by the energy of the photoelectron relative to the first target state, as was shown in Eq.(2.6).

The calculation of the hamiltonian matrix elements involves very complicated mathematical procedures and we will not discuss them here. Basically, the elements are expressed in terms of a set of integrals of bound and channel orbitals generated by using the **NONH** program. The channel orbitals are still unknowns so they are expanded in terms of B-spline functions. For large systems, the integral list generated by the NONH program can be very large, computation of the matrix elements can be very time consuming, thus a wise algorithm must be used for efficiently handling this list.

Finally we need to deal with the problem of orthogonality requirements. If channel k is to be orthogonal to orbital $P(r)$, by introducing a Lagrangian multiplier and imposing the orthogonal condition, we can rewrite the system as [5]

$$\begin{pmatrix} (\mathbf{H} - E\mathbf{S}) & \mathbf{b} \\ \mathbf{b}^t & 0 \end{pmatrix} \begin{pmatrix} c \\ \lambda \end{pmatrix} = 0 \quad (2.15)$$

where λ is the Lagrangian multiplier, \mathbf{b} is a vector, it is zero everywhere except at the rows that corresponds to channel k , where $\mathbf{b} = \mathbf{B}\mathbf{b}'$, and \mathbf{b}' is the spline expansion coefficients of the orbital $P(r)$. So one more equation and one scalar element (λ) are added to the equation for each orthogonality condition.

Up to now, we have set up the interaction matrix and at this point, we are ready to solve this system for the expansion coefficients.

The boundary condition

It is very important to apply the appropriate boundary conditions to the channel orbital functions. First of all, the orbital wave function $P(r)$ should be zero at $r = 0$. Then, we must also require $P(r = r_{max}) = 0$ for closed channel orbitals. Whether a channel is open or close depends on the energy of the system. From Eq.(2.6) we learn that for a specified channel associated with target i , it is an open channel if $E - E_{t_i} > 0$ and closed channel otherwise.

CHAPTER III

CONTINUUM STATE WAVE FUNCTION AND ITS APPLICATION

In this chapter, we describe the inverse iteration approach for the continuum problem, discuss the calculation of wave functions, the normalization of the wave functions, and the calculation of physical properties from these wave functions.

Multi-channel inverse iteration approach

We have already shown that the problem of solving the Schrödinger equation

$$(H - E)\Psi = 0 \tag{3.1}$$

can be converted approximately to the problem of solving a system of linear equation

$$AC = 0 \tag{3.2}$$

where A is the matrix in Eq.(2.15) with appropriate boundary conditions applied.

When E is an eigenvalue of H , the matrix A will become singular as the accuracy increases. In an approximate case, the energy E which satisfies Eq.(3.2) cannot be exactly equal to an eigenvalue of the H which satisfies Eq.(3.1) but will be very close to one of the eigenvalues of H which corresponds to the smallest eigenvalue of A . So for the continuum-state problem with a given energy E which is an eigenvalue of H , the problem of solving the system $AC = 0$ for the expansion coefficient C of the wave function turns out to be a problem of finding the eigenvector corresponding to the smallest eigenvalue of A (see references [1, 4] for a detailed description). An investigation by Brosolo, Decleva, and Lisini[8] showed that it is more stable to solve

$A^t AC = 0$ instead of $AC = 0$. The inverse iteration approach was shown to be very efficient in dealing with this problem[1, 5].

In the multi-open channel case, we need to determine several degenerate solutions for each given energy E . The number of independent solutions to be determined for each energy equals the number of open channels. In the approximate case, the degeneracy is broken because the matrix A is not strictly singular. We can solve them by finding the eigenvectors corresponding to the smallest eigenvalues of A . We repeatedly perform inverse iteration for a solution and orthogonalize it to the ones already obtained. Because the overlap matrix S is not diagonal, the orthogonality between solutions $C^{(m)}$ and $C^{(n)}$ should be carried out as

$$C^{(m)t} SC^{(n)} = \delta_{mn} \quad (3.3)$$

On the other hand, however, the solutions obtained here are still not the physical solutions. We will need to transform them to the K-matrix normalized form. As long as the solutions obtained here are linearly independent, we can expect that the final physical solution should have the same form, independent of the orthogonality schemes. Because of this, we can discard the S matrix when imposing the orthogonalization requirements among the solutions. To confirm this claim, we list in Table 4.2 through Table 4.4 the physical results obtained under the two different orthogonality schemes.

Normalization of wave function

A procedure combining the WKB method [9, 10] with the spline basis is used to determine the normalization and phase shift of the continuum orbitals. To normalize

the open channel functions, we need to match the un-normalized channel functions with Coulomb functions in the asymptotic region. The radial equation for an electron under a Coulomb potential with effective nuclear charge Z_{eff} is

$$y(r)'' + w(r)y(r) = 0 \quad (3.4)$$

where

$$w(r) = k^2 + 2Z_{eff}/r - l(l+1)/r^2 \quad (3.5)$$

with $k^2/2$ for the energy (in a.u.) of the electron and l for its orbital angular momentum.

The radial function $y(r)$ can be written as

$$y(r) = \frac{1}{\zeta^{1/2}} \sin \phi(r) \quad (3.6)$$

In the asymptotic region , $\zeta(r)$ satisfies the equation,

$$\zeta = \left[w(r) + \zeta^{1/2} \frac{d}{dr^2} \zeta^{-1/2} \right]^{1/2} \quad (3.7)$$

A number of methods have been proposed to solve the above equation and determine the phase function $\phi(r)$ and normalization of the wave function [11, 12, 13]. Here we use the Maple symbol manipulation package [14] and determine the iterates analytically up to 4 iterations [15]. With a sufficiently large r value, the iteration converges to an error of less than 10^{-9} .

Having $\zeta(r)$ determined at a given large r value, we can determine the phase function $\phi(r)$ from Eq.(3.6), which gives

$$\tan \phi(r) = \zeta / \left(\frac{y'}{y} + \frac{\zeta'}{2\zeta} \right) \quad (3.8)$$

where $y'(r)$ and $\zeta'(r)$ are the derivatives of $y(r)$ and $\zeta(r)$, respectively, at the given r value.

The energy normalized regular and irregular Coulomb functions can be written as

$$F(r) = \sqrt{\frac{2}{\pi\zeta}} \sin \phi(r) \quad (3.9)$$

$$G(r) = \sqrt{\frac{2}{\pi\zeta}} \cos \phi(r) \quad (3.10)$$

These are then used to match the un-normalized radial channel function at the given r value, Let $\overline{P}_{ij}(r)$ be the j -th solution for the i -th channel, for a given energy, we have

$$\overline{P}_{ij}(r) = F_i(r)A_{ij} + G_i(r)B_{ij} \quad (3.11)$$

or

$$\overline{P} = FA + GB \quad (3.12)$$

in matrix form, where A and B are coefficient matrices, F and G are diagonal matrices defined as

$$F_{ij} = F_i(r)\delta_{ij} \quad (3.13)$$

$$G_{ij} = G_i(r)\delta_{ij} \quad (3.14)$$

Multiplying Eq.(3.12) on the right by A^{-1} , we get the K-matrix normalized channel functions

$$\tilde{P} = FI + GK \quad (3.15)$$

where

$$\tilde{P} = \overline{P}A^{-1} \quad (3.16)$$

and K is the reaction matrix

$$K = BA^{-1}. \quad (3.17)$$

It should be mentioned that, care must be taken when calculating the K matrix. When the phase shift of a certain channel approaches $\pi/2$, the matrix A^{-1} will be singular, this will lead to serious numerical errors, and cause pseudo resonances when K is used. In this case, we should calculate $\mathbf{K}^{-1} = AB^{-1}$ instead of calculating K .

The scattering matrix \mathbf{S} is defined as [16]

$$\mathbf{S} = \frac{(1 + i\mathbf{K})}{(1 - i\mathbf{K})} \quad (3.18)$$

The final state should be subject to the boundary condition of an incoming wave. Then the wave function should be normalized according to the \mathbf{S} matrix,

$$P = FI + GS \quad (3.19)$$

For the one open channel case, this differs from the K -matrix normalized wave function by only a fixed constant, so we can simply use the latter as our normalized wave function. For the multi-channel case, however, the K -matrix normalized wave function no longer represents the physical situation. The energy normalized channel wave function P subject to the final physical boundary condition (Eq.(3.19)) can be written as

$$P = \overline{P}C \quad (3.20)$$

where C is the normalization matrix,

Let $\overline{\Psi}_j$ be the j -th solution of the un-normalized final state wave function, \overline{W}_{ij} the weight coefficients of the i -th bound perturbors corresponding to $\overline{\Psi}_j$. We can rewrite Eq.(2.3) as

$$\overline{\Psi}_j = \sum_{i=1}^{M_p} \phi(\alpha_i) \overline{W}_{ij} + \sum_{i=1}^{M_c} \overline{\varphi}_{ij} \quad (3.21)$$

where $\overline{\varphi}_{ij}$ is the j -th un-normalized wave function of the i -th channel state. From Eq.(3.20), we can get the normalized channel state wave function as

$$\varphi = \overline{\varphi}C \quad (3.22)$$

Similarly, we can get the normalized perturber weight, as

$$W = \overline{W}C \quad (3.23)$$

Substituting Eq.(3.22) and Eq.(3.23) into Eq.(3.21), we get the j -th normalized final state wave function as

$$\Psi_j = \sum_i \overline{\Psi}_i C_{ij} \quad (3.24)$$

Let \overline{d}_j be reduced dipole matrix elements between the initial state (Ψ_0) and the j -th un-normalized final state

$$\overline{d}_j = \langle \overline{\Psi}_j | T | \Psi_0 \rangle \quad (3.25)$$

then from eq.(3.24) we get the normalized reduced dipole matrix elements for the j -th state as

$$d_j = \sum_i \overline{d}_i C_{ij} \quad (3.26)$$

We have two equivalent methods to calculate the C matrix. It can be calculated by means of the eigenvectors \mathbf{U} and the eigenvalues $\tan \delta$ of the K matrix (δ is called diagonal phase shift), or K^{-1} matrix

$$\left\{ \begin{array}{l} U^{-1}KU = \tan \delta \\ C = A^{-1}Q \end{array} \right\} \text{ or } \left\{ \begin{array}{l} U^{-1}K^{-1}U = (\tan \delta)^{-1} \\ C = B^{-1}Q \end{array} \right\} \quad (3.27)$$

where

$$Q_{ij} = \sum_k U_{ik} U_{jk} \cos(\delta_k) e^{-i\delta_k} \quad (3.28)$$

or by means of \mathbf{A} and \mathbf{B} matrices [18, 19],

$$C = (A + iB)^{-1} \quad (3.29)$$

Let $C = X + iY$, then, with Eq.(3.29) we have

$$(X + iY)(A + iB) = I \quad (3.30)$$

or,

$$XA - YB = I \quad (3.31)$$

$$XB + YA = 0 \quad (3.32)$$

If A^{-1} is not singular, we have

$$K = BA^{-1} \quad (3.33)$$

$$X = (A + KB)^{-1} \quad (3.34)$$

$$Y = -XK \quad (3.35)$$

otherwise,

$$K^{-1} = AB^{-1} \quad (3.36)$$

$$Y = -(B + K^{-1}A)^{-1} \quad (3.37)$$

$$X = -YK^{-1} \quad (3.38)$$

Cross section and angular distribution

The photodetachment cross section (in a.u.) is defined as

$$\sigma = 4\pi^2\alpha\omega |\langle \Psi_E | T | \Psi_0 \rangle|^2 \quad (3.39)$$

where α is the fine-structure constant, $\omega = E - E_0$ is the photon energy, which is defined as the energy difference between the final state and the initial state. Ψ_0 and Ψ_E are the initial and final state wave function, respectively, represented in terms of the multi-configuration and/or multi-channel states under LS coupling. By using the Wigner-Eckert theorem, summing over the magnetic quantum numbers for the final state, and averaging over those of the initial state, we can get the cross section for each final state in terms of the reduced matrix elements of the transition operator T_μ^λ

$$\sigma = \frac{4\pi^2}{2\lambda + 1} \alpha \omega \left| \langle \Psi_E(LS) \| T^\lambda \| \Psi_0(L_0S) \rangle \right|^2 / (2L_0 + 1) \quad (3.40)$$

with $\lambda = 1$ for a dipole transition. The dipole transition operators in length and velocity form are (in a.u.)

$$\begin{aligned} T_L^1 &= \sum_j \vec{r}_j \\ T_V^1 &= \sum_j \frac{\nabla_j}{i\omega} \end{aligned} \quad (3.41)$$

Under the non-relativistic limit, the total cross section is simply the sum of the cross sections for all final states.

When a resonance appears, its position E_r and width Γ can be determined from the cross section. For a Feshbach resonance, it is determined by fitting the total photodetachment cross section $\sigma(E)$ by the many-channel Fano-Cooper formula [20]

$$\sigma(E) = \sigma_0 [1 + a(E - E_r)] \left[1 - \rho^2 + \rho^2 \frac{(q + \epsilon)^2}{1 + \epsilon^2} \right] \quad (3.42)$$

with

$$\epsilon = 2(E - E_r)/\Gamma \quad (3.43)$$

where a linear background $\sigma_0[1 + a(E - E_r)]$ is assumed in the resonance region. σ_0 is the background cross section at E_r and a is a parameter.

For a sharp resonance near threshold, the cross section can be well represented by the product of the Wigner threshold law and the Breit-Wigner resonance formula [21, 22]

$$\sigma_l(E) \sim \frac{(E - E_t)^{l+1/2}}{(E - E_r)^2 + (\Gamma/2)^2} \quad (3.44)$$

where l is the orbital angular momentum of the photoelectron associated with the open channel which produces the sharp resonance, σ_l is the partial cross section via this channel, E_t is the corresponding threshold (target) energy. If the cross sections via all other non-resonance channels can be regarded as linear in the resonance region, then the resonance position and width can be obtained by fitting the total cross section

$$\sigma_{tot}(E) = \sigma_0[1 + a(E - E_r)] \left[1 + b \frac{(E - E_t)^{l+1/2}}{(E - E_r)^2 + (\Gamma/2)^2} \right] \quad (3.45)$$

The angular distribution asymmetry parameter β of the photoelectron, according to Fano and Dill [23, 24], is defined in terms of the following weighted average of the partial cross section $\sigma(j_t)$ of all the angular momentum transfer j_t :

$$\beta = \frac{\sum_{j_t} \sigma(j_t) \beta(j_t)}{\sum_{j_t} \sigma(j_t)} \quad (3.46)$$

where $\beta(j_t)$ is the asymmetry parameter for angular momentum transfer j_t , which is

$$\max(|L_0 - L_c|, |l - 1|) \leq j_t \leq \min(L_0 + L_c, l + 1) \quad (3.47)$$

where L_0, L_c and l are the orbital angular momentum of the initial state, the final state target (or core) and the photoelectron, respectively.

The $\sigma(j_t)$ and $\beta(j_t)$ for each j_t are determined from the reduced dipole matrix elements as [23, 24, 25]

$$\begin{aligned} \beta_{fav}(j_t) &= \frac{(j_t + 1)|S_{j_t+1}(j_t)|^2 + (j_t - 1)|S_{j_t-1}(j_t)|^2 - 3\sqrt{j_t(j_t + 1)}[S_{j_t+1}(j_t)S_{j_t-1}^+(j_t) + c.c.]}{(2j_t + 1)(|S_{j_t+1}(j_t)|^2 + |S_{j_t-1}(j_t)|^2)} \\ \sigma_{fav}(j_t) &= \frac{4}{3}\pi^2 \alpha E \frac{2j_t + 1}{2L_0 + 1} [|S_{j_t+1}(j_t)|^2 + |S_{j_t-1}(j_t)|^2] \end{aligned} \quad (3.48)$$

for parity favored j_t , and

$$\begin{aligned}\beta_{unfav}(j_t) &= -1 \\ \sigma_{unfav}(j_t) &= \frac{4}{3}\pi^2\alpha E \frac{2j_t + 1}{2L_0 + 1} |S_{j_t}(j_t)|^2\end{aligned}\quad (3.49)$$

for parity unfavored j_t .

$S_l(j_t)$ is a reduced matrix defined as

$$S_l(j_t) = e^{-i(\delta_l - l\pi/2)} \sum_L \sqrt{2L+1} \begin{Bmatrix} L_c & l & L \\ 1 & L_0 & j_t \end{Bmatrix} \langle \Psi_E \| T^1 \| \Psi_0 \rangle \quad (3.50)$$

where δ_l is the Coulomb phase shift of the radial channel wave function, L is the angular momentum of the final state.

CHAPTER IV

DESCRIPTION OF THE PROGRAM PACKAGES

First we state the design and implementation strategy for the program packages to achieve the required tasks. Then we discuss the structure and usage of these packages: **CHMAT** is the package that set up the interaction matrix. **INVPHOTO** is the package that solves for the wave function and calculates the physical properties. **TOOL** is a supporting program that analyzes data, prepares data for plotting, calculates some physical properties, and so on. A set of common libraries must be involved to support the above packages.

Program design and implementation strategy

Basically there are significant distinctions between scientific research software design and commercial software design. The following strategies are followed in designing the present program packages:

- The software to be designed is not a product, it's just an intermediate state of scientific research, and basically it was designed for use only within the research group though it may eventually become a part of a common library. So usually, formal documentation will be omitted.
- A program that runs correctly does not mean it can give satisfactorily physical results. So it happens from time to time that a program or part of a program was implemented and then discarded because it can not achieve desired results.

Based on this, we cannot follow a formal design phase to implement the codes. The usual way is to build it to solve the simplest but physically interesting problems, then extend it to a more general case.

- As long as a program runs correctly, the most important factors we consider are speed and memory. A typical run in our atomic structure calculation takes several days to several weeks, and we always have good physical problems that will fill all the memory of a computer, and extensive use of virtual memory is absolutely unacceptable. It is crucial to make the program run fast and use memory efficiently.
- The current task is to extend the existing program packages, so we will reuse the original program structure and code as much as we can. Also because future extension is still possible, we must try as much as possible to make the code reusable and extendable.

The CHMAT program package

This program reads in the B -spline parameters, sets up the B -spline basis, then, reads in the configuration list of the wave function (**cfg.inp**) and the orbital wave functions of the fixed orbitals (**wfn.inp**) from disk. The orbital wave functions are then converted into B -spline expansions. Orthogonal requirements between orbitals are set up. The integrals and coefficients of the energy expansion of the system is then read from the **xint.lst** file and the values of the integrals are calculated. Based on the above preparation, the program begins to calculate the interaction matrix. The target energies for all channels and the bound-bound interaction matrix

elements are calculated first and saved in a disk file. Then for each channel orbital, the channel-bound and channel-channel interactions are carried out and saved. Finally, the Lagrange multiplier effects are added to the matrix file. Because the integral list and the interaction matrix consumes most of the memory, manipulating them becomes an important task of the program.

The schematic structure of the program is given in Figure 4.1.

The INVPHOTO program package

This program package reads in the output data files of **CHMAT** and performs the following tasks:

- multi-channel inverse iteration for each given energy. This stage costs most of the computation time. Different algorithms are considered for matrices of different sizes. Basically complete LU decomposition is used for a matrix with dimension less than 2000, and sparse matrix techniques are used for large matrices. The solutions obtained from this stage are saved to disk file for further use.
- wave function normalization. This part becomes much more complicated for multi-open channel cases.
- photoionization cross section and angular distribution calculation. A list of dipole matrix elements integrals are read from disk file and calculated for each energy value, so this part can also be time consuming.

A schematic structure of the program is shown in Figure 4.2.

The TOOL program package

The **TOOL** package consists of many small programs which perform some simple tasks on data. The main tasks include:

- add an extra label to the electron orbitals in the **clist**, for example, change $1s$ to $1s1$.
- add a channel electron orbital (ks , for example) to the configuration list of an N electron target state (3P , for example) to form the configuration list of an $N + 1$ electron state (4P , for example).
- condense and sort a configuration list.
- select configurations with certain orbitals or targets.
- form configuration list file with weight coefficients from **CI** program package **GBRCI**.
- generate a set of B -spline functions and their derivatives.
- organize, sort, and interpolate data.
- analyze the **photo.out** file from **INVPHOTO**.
- analyze the **dipole.out** file from **INVPHOTO**, and calculate the angular distribution parameter.
- analyze the **weight.out** file from **INVPHOTO**, classify the weight coefficients.
- analyze the **wfn.out** files in **MCHF** output format.

Common libraries

The following libraries are involved to support the above three packages:

- **ang**: routines to perform angular momentum operations.
- **comspl**: basic spline related routines supporting the spline-Galerkin and inverse-iteration.
- **eispk, linpk, lapack**: standard packages for linear algebra and eigenvalue problems.
- **radspl**: routines to perform radial orbital integration and operation using splines.
- **spl**: the basic routines to generate spline functions.
- **dyn**: routines for dynamic memory allocation, reallocation, and deallocation for various operating systems.

Program usage

The steps to be followed when using the **CHMAT-INVPHOTO** program package are as follows:

- 1) Prepare the configuration list (**clist**). The list consists of two parts: the perturber-state configurations which can be generated via **LSGEN**[6] and the channel configurations which are obtained by attaching the channel electron states to the corresponding target states by using **TOOL**. The channel configurations appear after the perturber-state configurations in the **clist** with

target energies in increasing order. The non-default orthogonality constraints are put at the end of **clist** file.

- 2) Put the orbital wave functions for fixed orbitals in file **wfn.inp** which is in **MCHF** output format. If this file is missing, a hydrogenic-like wave function will be generated automatically.
- 3) Run **XNONH** (the **NONH** package[6] with unformatted data storage) to generate integral list **xint.lst**.
- 4) run **XCHDYN96** , the new version of **CHMAT** with dynamic memory allocation.
- 5) Run **MLTPOL**[6] to generate dipole matrix element list (**mltpol.lst**). The initial state configuration list should be provided). If only the final state wave function is needed, skip this step.
- 6) Run **INVDYN96**, the new version of **INVPHOTO** with dynamic memory allocation.
- 7) Run **TOOL** to analyze data, calculate angular distribution, etc.

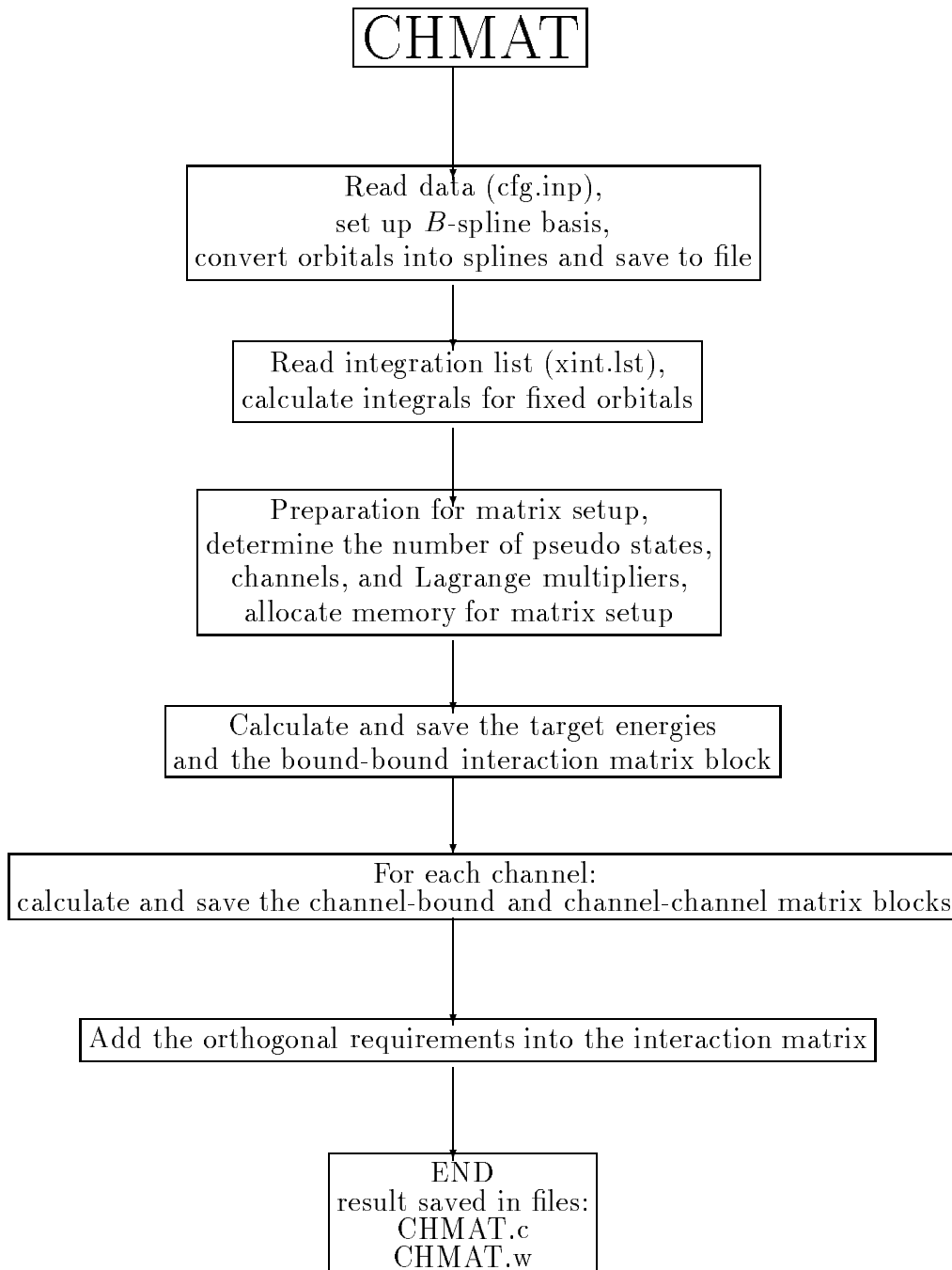


Figure 4.1: The schematic structure of the CHMAT program package

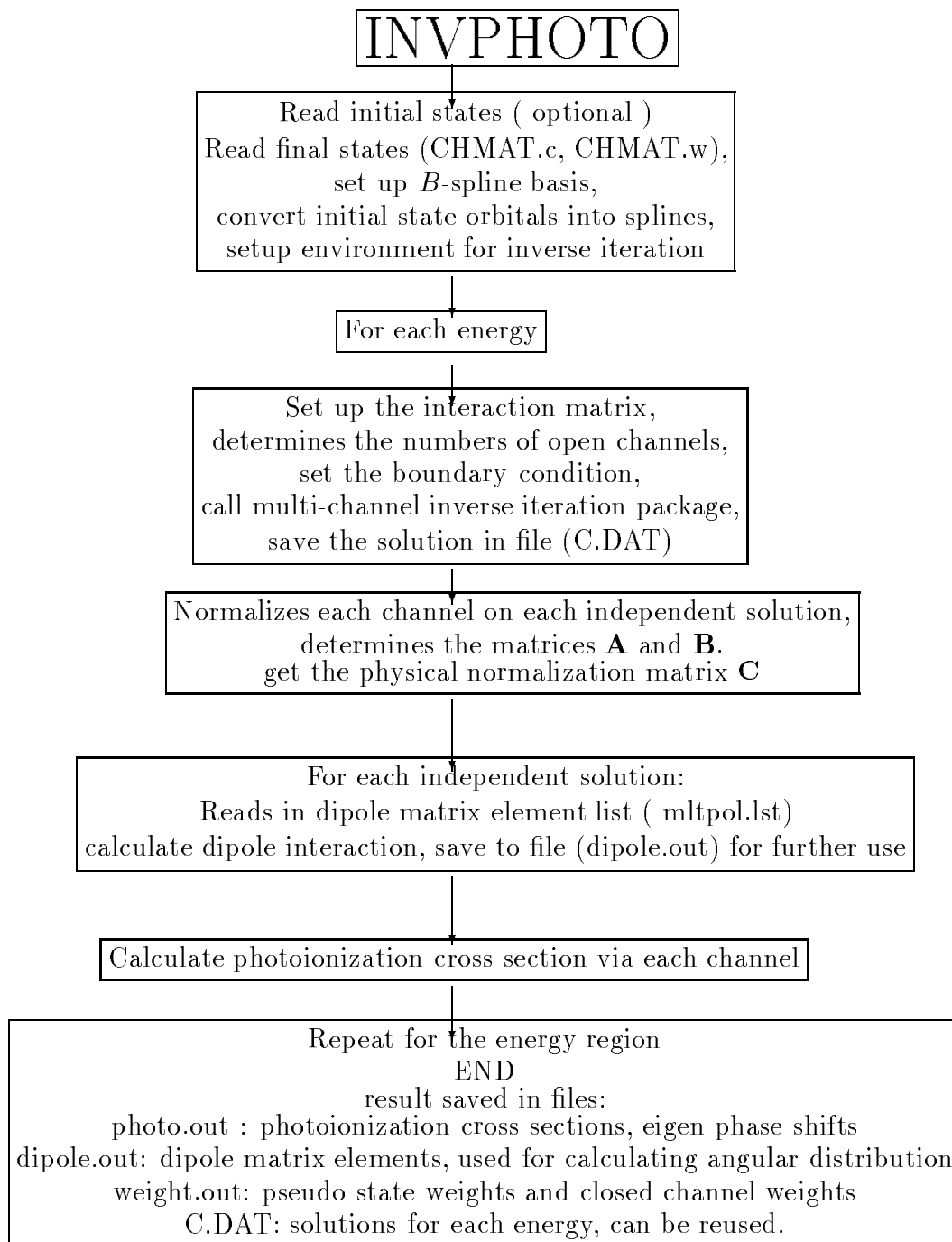


Figure 4.2: The schematic structure of the INVPHOTO program package

CHAPTER V

PROGRAM VALIDATION AND APPLICATION

This chapter consists of three parts. First, we describe methods for validating the program; then, we present a sample calculation for the photoionization process of the He atomic system; finally, we illustrate an application to the calculation of the He⁻ photodetachment cross section and angular distribution.

Program validation methods

There are many ways to check the correctness of the program. Here we illustrate an approach which incorporates the mathematical nature of the current problem. As we have explained in the earlier chapters, we can have non-orthogonal orbitals in the configuration list. Whether the orbitals are orthogonal or not, the final physical result should be the same. For example, we should always get the same energy for the same system. So if the program works correctly, it should produce identical results under different orthogonal schemes.

Consider the following sample configuration list of a two electron atomic system.

$$2s k p_1$$

$$2p k s$$

$$\langle k s | 2s \rangle$$

where $\langle k s | 2s \rangle$ means that the orbitals $k s$ and $2s$ are orthogonal to each other. In this case, we only require that $k s$ be orthogonal to $2s$ so that the two configurations are

orthogonal with each other. We do not need kp_1 and $2p$ to be orthogonal. Generally speaking, kp_1 can have a component parallel to $2p$ and a component orthogonal to it.

Let

$$kp_1 = 2p + kp$$

then

$$2skp_1 = 2s2p + 2skp$$

so we get the following configuration list

$$2s2p$$

$$2skp$$

$$2pks$$

$$\langle 2s|ks \rangle$$

$$\langle 2p|kp \rangle$$

These two lists are mathematically identical and thus should produce the same result. We can generate as many sample lists as we want to test our program. For example, for the He^- system, where there are three electrons outside of the atomic nucleus, the following sample configuration lists are mathematically identical,

$1s2p^2$	$1s2p^2$
$1s3p^2$	$1s3p^2$
$1s2pkp_1$	$1s2p3p$
$1s3pkp_2$	$1s2pkp_1$
$\langle 2p 3p \rangle$	$1s3pkp_2$
$\langle 2p kp_1 \rangle$	$\langle 2p 3p \rangle$

$$\begin{array}{ll}
\langle 3p|kp_2 \rangle & \langle 2p|kp_1 \rangle \\
& \langle 2p|kp_2 \rangle \\
& \langle 3p|kp_2 \rangle
\end{array}$$

If the program can pass all these tests, we have confidence in the belief that it behaves correctly, even though we do not know whether or not it will produce our desired physical result — this is not the program’s responsibility.

Another way to validate the program is to compare it to the MCHF program. The CHMAT program package expands the channel orbitals and sets up the interaction matrix, but lets the expansion coefficients be determined by the INVPHOTO program. If we set expansion coefficients of the channel orbitals manually to those of orbitals we already know, for example, set the coefficients of kp to those of $3p$, or $4p$, \dots , then, we can calculate the energy of the interaction matrix, and the result should be the same as we get from an MCHF calculation.

Test cases

A test calculation is made for the photoionization of He . First of all, we want to compare our results with those of Decleva et al[26], where new numerical data are listed. Detailed results are listed in Table 5.1. We see, our results are in complete agreement with those of Decleva et al.

Next we want to check the difference of the results under different orthogonality requirements. The results listed in Table 5.1 are the case where independent solutions are orthogonalized without an overlap matrix. Another case, which seems to be more physical, is to include the overlap matrix in the orthogonal requirements (see

Eq.(3.3)).

Because the purpose of the current orthogonal requirements is to ensure the independence of the multi-channel solutions, no matter what orthogonal algorithms are imposed, the solutions still need to be transformed to meet the physical requirement. So it seems that the orthogonal algorithms employed here will not affect the final physical results.

To support the above claim, we perform some test calculations. Results from these two cases are listed in Table 5.2 through Table 5.4.

In Table 5.2 and Table 5.3, we list the phase shift and the K-matrix for $E=68$ eV. It is clear that the phase shifts of the individual channels are different for the two orthogonality schemes, but the K-matrix elements are the same, the difference is less than 10^{-12} , which can be considered as machine accuracy. In Table 5.4, We list the partial and total cross sections, for $E = 68$ eV, and $E=75$ eV, respectively, we can see that the results are identical for the two different orthogonal schemes.

In the above calculation, we get the independent solution for each energy by searching the eigenvectors of the smallest eigenvalues of the matrix $A^t A$.

Applications in atomic photodetachment processes

The study of negative atomic ions are of great research interest in both experimental and theoretical aspects. The diffusive nature of a negative ion becomes a real challenge for accurate theoretical calculations. An example of such system is He^- . The photodetachment of this system has always been an active research topic, but results from experiments and earlier calculations differ considerably, as we will see later in Table 5.5.

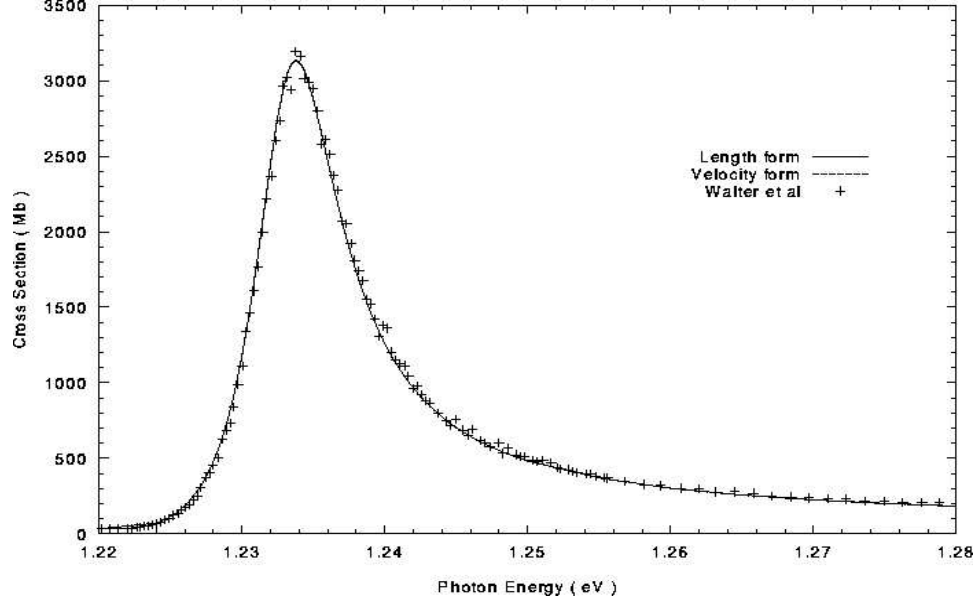


Figure 5.1: Comparison of the present calculation with the experimental data of Walter, Seifert, and Peterson[22] in the region of the $1s2p^2$ sharp resonance. The experimental data are scaled by a factor of $5/9$ because of the reason described in Ref[22] . We can see that the agreement is really impressive.

The current methods and the program packages have been used successfully for the study of the multi-channel photodetachment properties of negative ions. Systems studied include He^- , Be^- , and B^- . The nuclear charge in these systems are 2, 4, and 5 , respectively. Results for the He^- anion have been published[27]. Results for the other negative ions will also be submitted. A comparison of the present calculation with the most recent experiment are shown in Figure 5.1. Comparison of resonance parameters are shown in Table 5.5.

In studying the photodetachment processes, we obtained an excellent agreement with the most recent experimental data as shown in Figure 5.1. We found some resonances which were never reported before, as shown in Table 5.6. These new resonances have stimulated the interest of several experimental physicists in designing sophisticated experiments to search for these resonances.

Table 5.1: Total photoionization cross section (Mb) for the Helium $1S$ state. The spline parameters are: $h = 1/8, h_{max} = 3/8, R_{max} = 40., k = 8$, with 16 channels. The dimension of the matrix is 2052

E(eV)	σ_L^a	σ_V^a	σ_L/σ_V	σ_L^b	σ_V^b
24.6	7.3212	7.2299	1.013	7.32	7.23
	7.3199	7.2277			
30.0	5.3686	5.2902	1.015	5.37	5.29
	5.3687	5.2890			
40.0	3.1995	3.1413	1.019	3.20	3.14
	3.2004	3.1418			
50.0	2.0711	2.0268	1.022	2.07	2.03
	2.0720	2.0265			
68.0	1.1291	1.1048	1.022	1.13	
	1.1305	1.1047			
75.0	0.8896	0.8691	1.024	0.891	0.869
	0.8908	0.8690			

^a Initial state wave function is obtained from MCHF approach. Two cases are considered, 1) MCHF expansion includes orbitals up to $n=5$. 2) orbitals up to $n=8$ are included. The results are listed in the first and second row respectively, for each given energy.

^b Results of Decleva et al, JPB27, 1994

Table 5.2: Phase shift matrix under different orthogonality scheme. 1) without overlap matrix, 2) with overlap matrix. The photon energy is 68 eV

1.9252067	1.9252452	1.9235851	0.0035257
0.1169782	1.0816623	0.5785006	0.3665995
0.1554529	0.3084951	0.5902616	0.3708610
1.7032326	1.8509464	0.1817685	1.2035732
1.9252067	1.9252440	1.9237256	0.0018886
0.1169782	1.0625289	0.5755221	0.3967330
0.1554529	0.3040385	0.5947699	0.4004716
1.7032326	1.8528694	0.1796742	1.2262278

Table 5.3: K-matrix under different orthogonality scheme. 1) without overlap matrix, 2) with overlap matrix. The photon energy is 68 eV

-0.008618893079	-0.153309443211	-0.026773301283	-0.110222360282
-0.153309772517	-3.539129145862	4.627657885142	-2.086843989106
-0.026771899867	4.627633170105	-4.596237914811	2.809315257858
-0.110222014633	-2.086830580313	2.809312470471	-1.746986689205
-0.008618893079	-0.153309443211	-0.026773301283	-0.110222360282
-0.153309772514	-3.539129145864	4.627657885142	-2.086843989108
-0.026771899869	4.627633170107	-4.596237914811	2.809315257859
-0.110222014632	-2.086830580314	2.809312470471	-1.746986689206

Table 5.4: Partial and total photoionization cross section (Mb) for the Helium 1S state. Degenerate solutions are obtained under two orthogonality algorithm: 1) without overlap matrix, 2) with overlap matrix. The spline parameters are the same as in Table 5.1. Initial state are from $n=5$ MCHF expansion. The photon energies are 68 eV and 75 eV, there are 4 open channels at 68 eV and 9 open channels at 75 eV. For each open channel, the first row in the table lists the results of case 1, the second row lists the results of case 2. We see the results of the two cases are identically the same.

	σ_L^a	σ_V	σ_L/σ_V	σ_L^b	σ_V	σ_L/σ_V
1s	1.0226828	0.9960742	1.027	0.7942761	0.7716402	1.029
	1.0226828	0.9960742	1.027			
2s	0.0328249	0.0341933	0.960	0.0258512	0.0277610	0.931
	0.0328249	0.0341933	0.960			
2ps	0.0509187	0.0527769	0.965	0.0329158	0.0348053	0.946
	0.0509187	0.0527769	0.965			
2pd	0.0226951	0.0217183	1.045	0.0214231	0.0197125	1.087
	0.0226951	0.0217183	1.045			
3s				0.0022348	0.0022220	1.006
3ps				0.0057438	0.0056393	1.019
3pd				0.0039267	0.0038972	1.008
3dp				0.0027120	0.0029039	0.934
3df				0.0004785	0.0005307	0.902
Total	1.1291215	1.1047627	1.022	0.8895619	0.8691121	1.024
	1.1291215	1.1047627	1.022	0.8895619	0.8691121	1.024

^a Results at 68 eV.

^b Results at 75 eV.

Table 5.5: The resonance parameters for the $1s2p^2\ ^4P$ sharp resonance are determined by fitting the total cross section to Eq.(3.45) in the energy region from 1.22 eV to 1.28 eV. Threshold energy was fixed in the fitting process. Other theoretical and experimental results are also listed for comparison.

	σ_R (Mb) ^a	$\sigma_R/\sigma_{E_0}^b$	E_r (meV)	Γ (meV)
with constant background ^b				
Length Form	3125.5	125.6	1232.91	7.067
Velocity Form	3132.6	128.4	1232.90	7.058
with linear background ^b				
Length Form	3125.5	81.1	1232.95	7.267
Velocity Form	3132.6	81.5	1232.95	7.264
Hazi and Reed[28]	2.4×10^3	~ 80	1232.2	7
Saha and Compton[30]	$\sim 10 \times 10^3$ ^c	~ 280 ^c	1231	7.5
Peterson et al[29]	7×10^3		1234.4	7.0
Peterson et al[21]	$(7.4 \pm 1.5) \times 10^3$		1232.9 ± 0.3	7.4 ± 0.3
Walter et al[22]	$(5.8 \pm 2.0) \times 10^3$	89 ± 5	1232.95 ± 0.07	7.16 ± 0.07

^a σ_R is the maximum cross section at resonance.

^b $\sigma_{E_0} = \sigma_0[1 + a(E_0 - E_r)]$ is the cross section at the threshold. In the case of constant background cross section, the parameter a is set to zero and thus $\sigma_{E_0} = \sigma_0$. For linear background, a is varied.

^c Values are taken from Table I of Ref.[22].

Table 5.6: The positions and widths of the Feshbach resonances below the $n = 3$ and $n = 4$ thresholds.

state	Length Form		Velocity Form	
	E_r (eV)	Γ (meV)	E_r (eV)	Γ (meV)
$1s3s4s\ ^4S$	2.95907	0.19	2.95908	0.18
$1s3p^2\ ^4P$	3.07470	37.37	3.07471	37.37
$1s3p4p\ ^4P$	3.26554	1.30	3.26547	1.31
$1s4p^2\ ^4P$	3.81142	28.19	3.81138	28.18
$1s4p5p\ ^4P$	3.94761	6.05	3.94754	5.97

CHAPTER VI

FUTURE DEVELOPMENT

The CHMAT-INVPHOTO packages are described in detail in the preceding chapters. Applications to real physical systems have achieved great success. This software package was initially designed to study atomic photoionization and photodetachment processes of two-electron systems, and has been extended by the present work to a general case of multi-electron systems. Because of the reason we will state later, this extended system is efficient for few-electron systems but not very efficient for many-electron systems with strong core-polarization. It is worthwhile to make further modifications and extensions. In the mean time, this package can also be extended easily to study other processes such as autoionization and electron impact excitation.

Study of many-electron systems with core polarization

For multi-electron systems, the core polarization might be an important effect in determining the accuracy of the theoretical calculation. The current software package deals with this effect by including the configuration interactions among the open shells and the closed shells. For many electron systems, this will lead to an extremely large configuration set which exceeds the speed and memory limits of the currently available computer resources. Another problem is that the current package requires orbitals of initial and final states be the same orbital set. This will lead to a very large orbital set for complicate systems. The following methods can be used to solve these problems:

- use different orbital sets for initial and final state wavefunctions. The **CHMAT-INVPHOTO** package can be kept unchanged, we only need a new version of **MLTPOL** to calculate the dipole matrix elements between initial and final states where overlap of non-orthogonal orbitals will be handled.
- represent the core polarization in terms of a polarization potential. The structure of the current program packages are still reusable but extension is needed for **CHMAT** package to calculate the matrix elements of the potential.

Study of atomic auto-ionization and autodetachment processes

Autoionization comes from the interaction of a discrete perturber, Ψ_b with energy E_b , and its adjacent continuum state, Ψ_k , and thus cause a resonance. The width of the resonance is defined as

$$\Gamma = 2\pi |V_{E_b}|^2 \quad (6.1)$$

where

$$V_{E_b} = \langle \Psi_b | H - E_b | \Psi_k \rangle \quad (6.2)$$

So, what we need to do is to calculate the matrix elements of the hamiltonian of the system between these components of a wave function which are the output of the **CHMAT-INVPHOTO** package.

Study of electron impact processes

Elastic scattering is one of the most important process in atomic collision. In this case an independent-channel approximation can be used and the mathematical complexity will be significantly reduced. The differential cross section can be written

as (in atomic unit)

$$\frac{d\sigma}{d\Omega} = |f(\theta)|^2 \quad (6.3)$$

where $f(\theta)$ is the scattering amplitude

$$f(\theta) = \frac{1}{k} \sum_{l=0}^{\infty} (2l+1) e^{i\delta_l} \sin \delta_l P_l(\cos \theta) \quad (6.4)$$

where $P_l(\cos \theta)$ is the l th Legendre polynomial, δ_l is the phase shift, and k is the electron momentum (in atomic unit).

The total cross section is

$$\sigma = \frac{4\pi}{k^2} \sum_{l=0}^{\infty} (2l+1) \sin^2 \delta_l \quad (6.5)$$

and the momentum transfer cross section is

$$\sigma_M = \frac{4\pi}{k^2} \sum_{l=0}^{\infty} (l+1) \sin^2(\delta_l - \delta_{l+1}) \quad (6.6)$$

So **CHMAT** can be used to set up the interaction matrix and **INVPHOTO** can still be used to solve the final state wave function and calculate the phase shift. We only need to code the above equations using the phase shift as input. All these extensions can be done very easily.

There are many cases where the independent-channel approximation becomes invalid and the cross section cannot be determined by the above equations. But the result of **CHMAT** and **INVPHOTO** are still usable. Since the detailed process is very complicated and involves too much physics, we will not discuss this issue here.

BIBLIOGRAPHY

- [1] C. Froese Fischer and M. Idrees, Comput. Phys. **3**, 53 (1989)
- [2] C. Froese Fischer, W. Guo, and Z. Shen, Int. J. Quantum Chem. **42**, 849(1992)
- [3] C. Froese Fischer and F.A. Parpia Phys. Lett. A **179**, 198(1993)
- [4] C. Froese Fischer and M. Idrees, J. Phys. B **23**, 679(1990)
- [5] T. Brage, C. Froese Fischer, and G. Miecnik, J. Phys. B **25**, 5289(1992)
- [6] C.Froese Fischer, Comput. Phys. Commum., **64**, 369(1991), and other related papers in the same issue.
- [7] C. deBoor, A Practical Guide to Splines (Springer, New York, 1978).
- [8] M. Brosolo, P. Decleva, and A. Lisini, Comput. Phys. Commun. **71**, 147(1992)
- [9] S.C.Miller,Jr. and R.H.Good, Jr., Phys. Rev., **91**, 174(1953)
- [10] M.J.Seaton and G.Peach, Proc. Phys. Soc., **79**, 1296(1962)
- [11] A.Burgess, Proc. Phys. Soc., **81**, 441(1963)
- [12] J.Stein, A.Ron, I.B.Goldberg, and R.H.Pratt, Phys. Rev. A, **36**, 5523(1987)
- [13] H.Liu, J. Xi, and B. Li, Phys. Rev. A, **48**, 228(1993)
- [14] B.W.Char, K.O.Geddes, G.H.Gonnet, M.B.Monagan, and S.M.Watt, A Tutorial Introduction of Maple, (Watcom Publications, Waterloo, Canada, 1990)
- [15] C.Froese Fischer, unpublished
- [16] U. Fano, Rep. Prog. Phys. **46**, 146(1983)
- [17] V. Jacobs, Phys. Rev. A **3**, 289(1971)
- [18] T.M.Luke, J. Phys. B **6**, 30(1973)
- [19] H.E.Saraph, Comp. Phys. Comm. **46**, 107(1987)
- [20] U. Fano and J.W.Cooper, Phys. Rev., **137**, A1364(1965)
- [21] J.R.Peterson, Y.K.Bae, and D.L.Huestis, Phys. Rev. Lett., **55**, 692(1985)
- [22] C.W.Walter, J.A.Seifert, and J.R.Peterson, Phys. Rev. A, **50**, 2257(1994)
- [23] D.Dill and U. Fano, Phys. Rev. Lett., **29**, 1203(1972)

- [24] U.Fano and D.Dill, Phys. Rev. A, 6, 185(1972)
- [25] S.T.Manson and A.F.Starace, Rev. Mod. Phys., 54, 389(1982)
- [26] P. Decleva, A. Lisini, and M. Brosolo, J. Phys. B 27, 4867(1994)
- [27] Jinhua Xi and Charlotte Froese Fischer, Phys. Rev. A 53, 3169(1996)
- [28] A.U.Hazi and K.Reed, Phys. Rev. A, 24, 2269(1981)
- [29] J.R.Peterson, M.J.Coggiola, and Y.K.Bae, Phys. Rev. Lett., 50, 664(1983)
- [30] H.P.Saha and R.N.Compton, Phys. Rev. Lett., 64, 1510(1990)

SOLUTION OF MULTI-CHANNEL CONTINUUM STATE PROBLEMS OF
MANY-ELECTRON ATOMIC SYSTEMS USING THE SPLINE-GALERKIN
AND INVERSE ITERATION APPROACH

JINHUA XI

Thesis under the direction of Dr. Charlotte Froese Fischer

The Spline-Galerkin and inverse iteration methods are applied to the treatment of general continuum state problems in theoretical atomic physics. A detailed investigation is performed by applying these methods to many electron atomic systems where multi-configuration target wave functions become necessary, and where multiple-open-channel solutions become much more complicated. Applications of the wave functions to the study of atomic properties are also investigated.

Based on an old version of the spline-Galerkin application package (CHMAT) and the inverse iteration package (INVPHOTO), we implement an extended version. The new version of the Spline-Galerkin program package employs B -splines as basis functions and uses the Galerkin method to set up a multi-channel interaction matrix. The channel configurations can be composed of multi-configuration targets. The inverse iteration program package uses the matrix and calculates the wave functions for open and closed channels by solving the generalized eigenvalue problem using the inverse iteration method. The inverse iteration algorithm is also extended to a general version for multi-open-channel cases. The algorithm and codes in the old version for

the normalization of channel wave functions are replaced by a general multi-channel normalization procedure. A new spline-WKB method is implemented to calculate the Coulomb functions in the asymptotic region. Function blocks are added to the program to calculate the physical properties for the multi-open-channel case. The programs are optimized and tested for correctness on both the IBM RISC/6000 system and the CRAY 2 system. Applications of these program packages to calculations for a number of atomic systems have achieved very good results.

Approved_____ Date_____